ACS APPLIED MATERIALS & INTERFACES

Research Article

www.acsami.org

Solution-Processed Poly(3,4-ethylenedioxythiophene) Thin Films as Transparent Conductors: Effect of *p*-Toluenesulfonic Acid in Dimethyl Sulfoxide

Smita Mukherjee,[†,⊥] Rekha Singh,[‡] Sreelekha Gopinathan,[§] Sengottaiyan Murugan,[‡] Suhas Gawali,[†] Biswajit Saha,[†] Jayeeta Biswas,[†] Saurabh Lodha,[†,∥] and Anil Kumar*[,†,‡,§]

[†]Centre of Excellence in Nanoelectronics, [‡]Department of Chemistry, [§]Centre for Research in Nanotechnology & Science, and [∥]Department of Electrical Engineering, Indian Institute of Technology Bombay, Mumbai 400076, India

Supporting Information

ABSTRACT: Conductivity enhancement of thin transparent films based on poly(3,4-ethylenedioxythiophene)−poly(styrenesulfonate) (PEDOT−PSS) by a solution-processed route involving mixture of an organic acid and organic solvent is reported. The combined effect of *p*-toluenesulfonic acid and dimethyl sulfoxide on spin-coated films of PEDOT−PSS on glass substrates, prepared from its commercially available aqueous dispersion, was found to increase the conductivity of the PEDOT−PSS film to ∼3500 S·cm^{-1} with a high transparency of at least 94%. Apart from conductivity and transparency measurements, the films were characterized by Raman, infrared, and X-ray photoelectron spectroscopy along with atomic force microscopy and secondary ion mass spectrometry. Combined results showed that the conductivity enhancement was due to doping, rearrangement of PEDOT particles owing to phase separation, and removal of PSS matrix throughout the depth of the film. The temperature dependence of the resistance for the treated films was found to be in accordance with one-dimensional variable range hopping, showing that treatment is effective in reducing energy barrier for interchain and interdomain charge hopping. Moreover, the treatment was found to be compatible with flexible poly(ethylene terephthalate) (PET) substrates as well. Apart from being potential candidates to replace inorganic transparent conducting oxide materials, the films exhibited stand-alone catalytic activity toward I^-/I_3^- redox couple as well and successfully replaced platinum and fluorinated tin oxide as counter electrode in dye-sensitized solar cells.

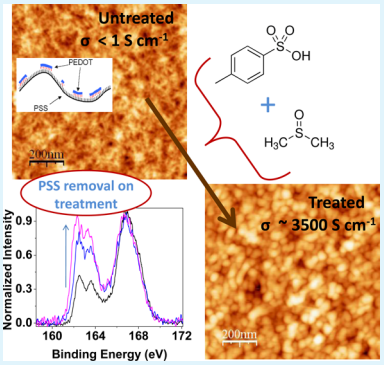

KEYWORDS: *PEDOT−PSS, transparent conducting polymer, conductivity enhancement, organic acid treatment, dye-sensitized solar cell*

I. INTRODUCTION

Transparent conductors (TCs) are optically transparent and electronically conductive materials. The demand for alternate TC materials, especially to replace the popularly used indium tin oxide (ITO),[1] is attributed to the vast optoelectronic applications[2,3] of TCs in diverse areas on one hand and to the drawbacks associated with ITO, such as problems of scarce indium on earth, high mechanical brittleness, expensive deposition techniques, and poor adhesion to organic and polymeric materials, on the other. Among the alternatives, transparent conducting oxides,[4,5] numerous solution-processable and printable candidates including metal nanowires[6,7] carbon nanotubes,[8−10] graphene,[11,12] and conducting polymers[13−17] are being actively investigated; the interest in organic transparent conductors is due to their ease of processing, ability to coat on curved surfaces, and resistance to dynamic stress.[14,16−18]

In this context, the conducting polymer poly(3,4-ethylenedioxythiophene) (PEDOT) doped with poly(styrenesulfonate) (PSS) (Figure 1a) has recently proved to be one of the most promising candidates for a next-generation TC material. PEDOT−PSS films have high transparency in the visible range, high mechanical flexibility, and excellent thermal stability.[19−21] It is commercially available as an aqueous dispersion from Heraeus[22] but has low conductivity (<1 S·cm^{-1}). Various methods have been designed for the conductivity enhancement of PEDOT−PSS thin films, of which, the solution processed route proved remarkable. The process essentially involves post-treatment of thin films of PEDOT−PSS by agents that dope or produce conformational changes in polymer chain and/or remove PSS that result in highly delocalized charge carriers and hence enhance its conductivity. Addition of various secondary dopants such as acids,[23−25] other organic compounds,[26−32] and ionic liquids[33] has been reported to enhance the conductivity of PEDOT−PSS thin films. Prior to discussing the recent reports in literature in more detail, a brief discussion on the quantitative parameters used to define any TC film may be worthwhile.

Received: July 6, 2014
Accepted: September 17, 2014
Published: September 17, 2014

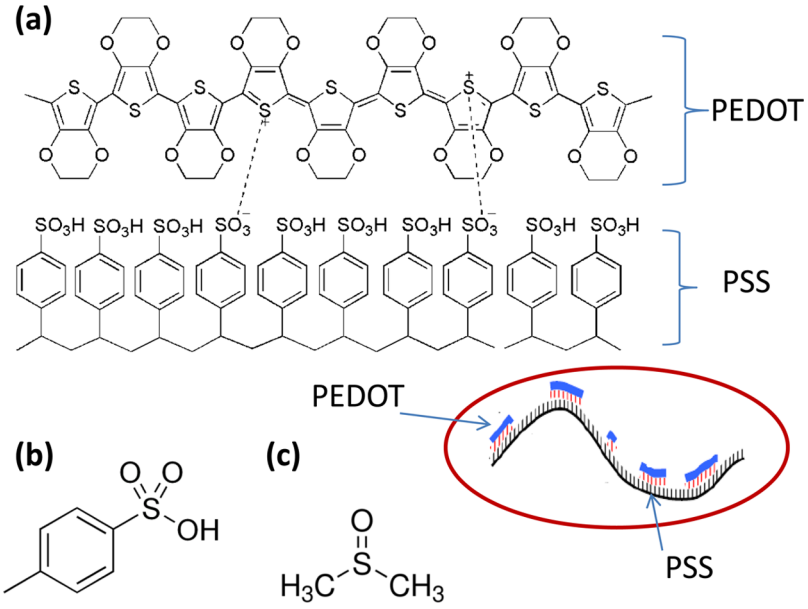

Figure 1. Schematic of (a) poly(3,4-ethylenedioxythiophene) doped with poly(styrenesulfonate) (PEDOT−PSS), (b) *p*-toluenesulfonic acid (PTSA), and (c) dimethyl sulfoxide (DMSO).

In general, the electronic conductivity (σ_{DC}) of a transparent conducting film is defined as

$$\sigma_{DC} = 1/(R_s Z) \quad (1)$$

where R_s is the sheet resistance and Z is the thickness of the film. Coupled with this, the value of the percentage transmittance of the film at 550 nm is quoted. Alternately, a material independent parameter, the σ_{DC}/σ_{OP} ratio (σ ratio), is usually used to quantify the efficiency of any transparent conducting material. It is defined as the ratio of electronic conductivity (σ_{DC}) to optical conductivity (σ_{OP}) and is related to the transparency (T) and sheet resistance (R_s) of the material as[34]

$$T = [1 + (Z_0/2R_s)\sigma_{DC}/\sigma_{OP}]^{-2} \quad (2)$$

where $Z_0 = 377\ \Omega$ is the impedance of free space. In the case of ITO-based TC, this ratio can be as high as 400,[35] whereas it is around 30 for graphene and carbon nanotube-based thin films.[21,36] As suggested by De and Coleman,[35] the σ ratio should be greater than 35 for most industrial applications, although some current-driven applications require more stringent σ values greater than 220. Again, applications such as liquid crystal displays (LCD) require σ values around 50, whereas other applications such as touch screens require a less stringent σ value of about 10.[36] However, since the σ ratio has a dramatic variation with small changes in transparency of the film[24] (Figure S1 in Supporting Information), one should keep in mind the individual values of sheet resistances and transparency of the films along with σ ratio. In this respect, it is generally agreed that TC materials must display a sheet resistance of $R_s < 100\ \Omega\cdot\square^{-1}$, coupled with transmittance of $T > 90\%$ in the visible region.[24,34−36] A detailed discussion on σ ratio, especially in relation to chemically and structurally altering PEDOT for transparent electrode applications, has also been reported by Hojati-Talemi et al.[37]

In this light, we proceed to discuss the recent results on conductivity enhancement as well as the values of σ ratio from literature. Among all secondary dopants used so far, addition of ionic liquid to PEDOT−PSS dispersion has been reported to yield the highest value of σ ratio of 185.[33] However, the conductivity of the thin film was ∼2100 S·cm^{-1}, a value less than that of ITO (∼3000 S·cm^{-1}). Furthermore, the stability of the PEDOT−PSS dispersion decreases significantly (phase separation happens in a few minutes) upon addition of ionic liquid and hence is of no practical use in large-area printing applications. This, along with the high cost of ionic liquid, makes this process less attractive. Treatment of PEDOT−PSS with acids, on the other hand, has been reported to enhance the conductivity to more than 3000 S·cm^{-1}, comparable to that of ITO, primarily by the removal of PSS from the film. Treatment with sulfuric acid at elevated[23] and room[38] temperatures yielded very high conductivity values of ∼3100 and ∼4400 S·cm^{-1}, respectively. However, the reported R_s values are typically >100 $\Omega\cdot\square^{-1}$ for a high transparency of 96%[23] and ∼46 $\Omega\cdot\square^{-1}$ for a transparency of 90%,[38] due to which the best value of σ ratio achieved is ∼72,[38] much less compared to that of ionic liquid treatment. Furthermore, treatment with sulfuric acid at elevated temperature, as well as use of the strong mineral acid in high concentrations, probably limits its application on organic substrates. The use of mild organic acids as secondary dopants has been recently reported. Methanesulfonic acid[25] at room temperature has shown very promising values of conductivity of ∼3300 S·cm^{-1} but with no mention of σ ratio. On the other hand, formic acid treatment yielded the second best reported σ ratio of 135 and was successfully carried out on large area flexible substrates. However, it was reported to have a much lower conductivity of ∼2000 S·cm^{-1}. Treatment of PEDOT−PSS with organic solvents, typically gives conductivity-enhanced values in the range 1000−1500 S·cm^{-1},[39−42] which is mainly caused by charge screening between PEDOT$^+$ and PSS$^-$ by high dielectric solvents.

Recently, a high conductivity value of 3400 S·cm^{-1} was measured in vapor-phase polymerization (VPP) PEDOT−Tos, where Tos represents the counterion tosylate (Figure 1), using a blend of an oxidant and an amphiphilic copolymer.[43] Even though the route is not solution-processed, the effect of the tosylate counterion in conductivity enhancement was signifi-

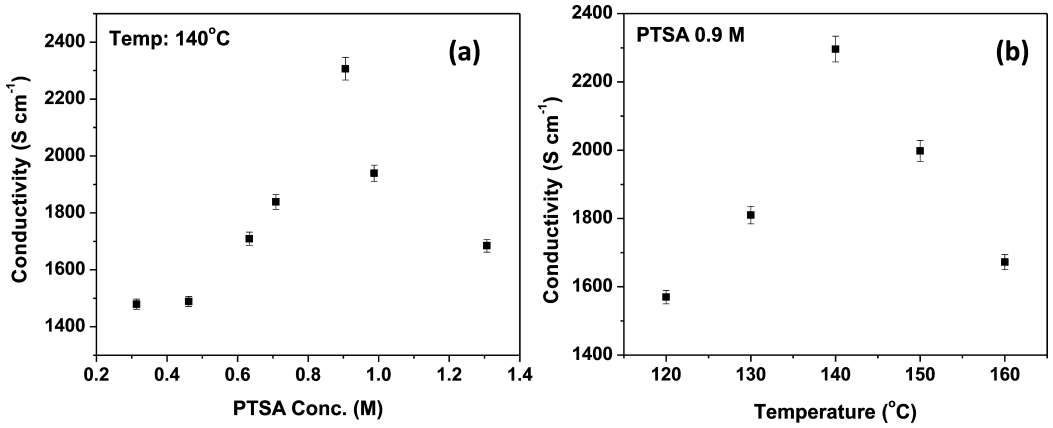

Figure 2. Variation of conductivity σ_{DC} with (a) concentration of PTSA and (b) temperature.

cant. In general, VPP technique has also gained attention in producing the insoluble polymeric material PEDOT into conductive, uniform thin films.[43,44] Even though a host of complementary techniques,[44,45] including inkjet printing and dip pen nanolithography (DPN), have shown the potential to pattern the oxidants used in the VPP process at or below the micrometer scale,[44] drawbacks remain as the conductivity values obtained in these processes are orders of magnitude lower compared to those of VPP with spin-coated oxidant layers, the latter exhibiting conductivities ~1000 $S{\cdot}cm^{-1}$.[44] Moreover, DPN is not appropriate for large area coatings.

We report the conductivity enhancement of thin films of PEDOT−PSS by a solution-processed route involving solution of *p*-toluenesulfonic acid (an organic acid containing the tosylate group; Figure 1b) in dimethyl sulfoxide (Figure 1c). The focus was to investigate the joint effect of the acid and solvent on spin-coated films of PEDOT−PSS as well as to note the role of the tosylate ion via solution-processed route. PEDOT−PSS films treated with this acid−solvent combination showed very high conductivity of ~3500 $S{\cdot}cm^{-1}$ with a high transparency of at least 94%. The σ ratio varied from 70 to 140, depending upon transparency of the films. Apart from the high conductivity and σ ratio, the present method is scalable to produce large-area thin films and is compatible with inorganic as well as organic substrates. Furthermore, successful fabrication of dye-sensitized solar cells (DSSCs) with these films replacing both platinum and fluorine-doped tin oxide (FTO) as the counter electrode, showed that along with being an alternative to inorganic oxide coatings, these exhibit significant catalytic activity as well. It must be mentioned that this combination treatment was used by Lee et al.,[46] who investigated thermoelectric properties of PEDOT−PSS. The conductivity value reported by them was, however, much lower at ~1300 $S{\cdot}cm^{-1}$.

In this paper, we report the combined effect of *p*-toluenesulfonic acid and dimethyl sulfoxide on spin-coated films of PEDOT−PSS on glass substrates, prepared from its commercially available aqueous dispersion. Apart from conductivity and transparency measurements, the films were characterized by a multitechnique approach involving Raman, infrared, and X-ray photoelectron spectroscopy along with atomic force microscopy and secondary ion mass spectrometry.

II. EXPERIMENTAL SECTION

PEDOT−PSS aqueous solution (Clevios PH1000) was purchased from Heraeus. The concentration of PEDOT−PSS was 1.3% by weight, and the weight ratio of PSS to PEDOT is 2.5 in solution. *p*-Toluenesulfonic acid (PTSA; Fisher Scientific, 99%), dimethyl sulfoxide (DMSO; Merck, 99.9%), sulfuric acid (Merck, 98%), and isopropyl alcohol (IPA; Merck, 99%) were used without further purification.

PEDOT−PSS films were prepared by spin-coating its aqueous dispersion on 1.0 × 1.0 cm^2 glass, poly(ethylene terephthalate) (PET), and ITO substrates. Glass substrates were precleaned successively with detergent, piranha solution [3:1 H_2SO_4 (98%)−H_2O_2 (30%) solution at 90 °C], deionized (DI) water, acetone, and IPA. ITO and PET substrates were precleaned in acetone and IPA. Thin films (<100 nm) of PEDOT−PSS were prepared following the thickness calibration curve of the spin-coater (Laurell) (Figure S2 in Supporting Information). Thick films (>100 nm) were prepared by multiple coatings of PEDOT−PSS solution. The organic acid−solvent treatment was performed by spin-coating 50 μL of a mixture of PTSA and DMSO solution on a PEDOT−PSS film. The films were baked at 140 °C for 5 min. These were thoroughly rinsed in IPA and finally dried at 140 °C for 15 min. For a set of films, this treatment was repeated multiple times on a single layer of PEDOT−PSS. An additional sulfuric acid treatment was carried out (both single and multiple times) on another set of films, after a one-time treatment with PTSA and DMSO solution. For each sulfuric aicd treatment, 1.5 M sulfuric acid was drop-cast at 140 °C for 2 min, thoroughly rinsed in DI water, and finally dried at 140 °C for 15 min.

The sheet resistance of the films was measured by a four-point probe (Lucas-Signatone) with a Keithley 2400 source meter. The film thickness was measured with an Ambios XP2 profilometer. For this, the film surface was scratched and measurements were done with a low stylus force of 0.05 mg. Transmittance was measured on a PerkinElmer UV−vis spectrometer (Lambda_750), with the bare substrate used as reference. Fourier transform infrared (FTIR) spectroscopy was done on a PerkinElmer Spectrum 100 at 4 cm^{-1} resolution in reflectance mode, with a mercury−cadmium−telluride (MCT) detector. Raman spectra were recorded on a Ramnor HG-2S spectrometer (Jobin-Yvon) with Ar laser (514.5 nm) at a resolution of 0.5 cm^{-1}. Atomic force microscopy (AFM) was done on a Nanoscope IV (Veeco Instruments) in tapping mode; cross-sectional scanning electron microscopy (SEM) was performed on a JEOL JSM-7600F field emission gun SEM. X-ray photoelectron spectroscopy (XPS) measurements were carried out by use of the PHI 5000 Versa Probe system (Ulvac-Phi Inc.). Time-of-flight secondary ion mass spectrometry (TOF-SIMS) measurement was carried out by use of a PHI TRIF V nanoTOF system (Ulvac-Phi Inc.) in negative polarity mode with an Au^+ ion analysis beam and a Cs^+ ion sputtering beam source. Depth profiling was carried out with an analysis ion beam current of 5 nA and a sampling area of 40 × 40 μm^2. Crater depth was measured at the end of the experiment with a profilometer. The low-temperature resistivity (LTR) measurement was carried out in a Quantum Design physical property measurement system, model 6000PPMS. Cyclic voltammetric studies were carried out with a CHI760D potentiostat in a

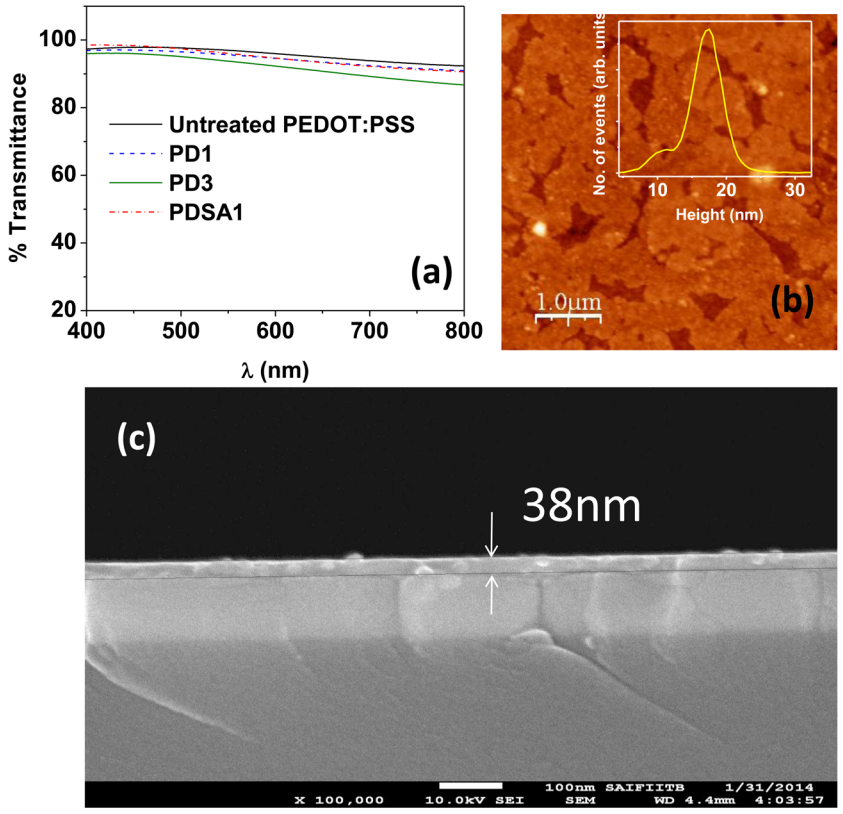

Figure 3. (a) UV−vis spectra of untreated PEDOT−PSS, PD, and PDSA films on glass; (b) AFM topographic image of PDSA5 film showing defect formation in films; (c) cross-sectional SEM image of PD3 film.

three-electrode configuration. Pt foil and Ag/Ag^+ were used as auxiliary and reference electrodes. LiI (10 mM), 1 mM I_2, and 0.1 M $LiClO_4$ in acetonitrile were used as electrolyte.

A. Fabrication of Dye-Sensitized Solar Cell. TiO_2 (Degussa P25, Germany) paste was prepared as per reported procedure[47] and deposited on FTO glass by the doctor blading method. TiO_2 film was sintered at 500 °C for 30 min to give a nanocrystalline film. The electrodes were immersed in dye solution [0.3 mM N719 (Solaronix)] for 24 h to achieve maximum dye loading. The counter electrodes used were sputtered platinum on FTO (in reference device) and PEDOT−PSS film treated with PTSA in DMSO (having $R_s \sim 20\ \Omega\cdot\square^{-1}$) on glass, with two predrilled holes on it. TiO_2 photoanode and counter electrode were assembled into a sandwich structure with Surlyn (Solaronix) as spacer. Electrolyte (0.1 M LiI, 0.05 M iodine, 0.6 M 1-methyl-3-propylimidazolium iodide, and 0.5 M 4-*t*-butylpyridine in acetonitrile) was filled into the gap through the hole drilled on the counter electrode, followed by sealing the hole with another piece of Surlyn and coverslip. The cell was characterized with a Keithley 2420 source meter under illumination (100 mW/cm^2) by a class A solar simulator (Newport Corp.).

III. RESULTS AND DISCUSSION

A. Conductivity Enhancement of PEDOT−PSS Film. PEDOT−PSS films on glass prepared from aqueous dispersion of Clevios PH1000 had a conductivity of 4×10^{-1} $S\cdot cm^{-1}$. The films were posttreated with a solution of PTSA in DMSO as described in the Experimental Section. The concentration of PTSA in DMSO, as well as the posttreatment baking temperature, was varied to get the optimum value of conductivity (Figure 2). The conductivity was found to be maximum for 0.9 M solution of PTSA in DMSO at a baking temperature of 140 °C. For single treatment with PTSA/DMSO solution, the conductivity of the film increased to~2300 $S\cdot cm^{-1}$ with a transparency of about 96%, giving a σ ratio of 127. With three treatments, there was further enhancement of the conductivity, increasing to ~3500 $S\cdot cm^{-1}$ with a transparency of about 94%, having a σ value of 77. Further treatment did not increase the conductivity but rather decreased it slightly to ~3200 $S\cdot cm^{-1}$ (Table S1, Supporting Information). The variation in conductivity enhancement with multiple treatments is discussed in detail later.

In order to systematically study the joint effect of acid and solvent, the results were compared with those for films individually posttreated with DMSO or an aqueous solution of PTSA. The sheet resistances of 100 nm PEDOT−PSS films, separately treated with DMSO or 0.9 M aqueous PTSA solution, were both ~200 $\Omega\cdot\square^{-1}$, as compared to that of 67 $\Omega\cdot\square^{-1}$ for the joint treatment. Moreover, aqueous PTSA-treated films developed white patches upon subsequent rinsing and drying, making the treatment ineffective. Films treated with other acids such as camphorsulfonic acid and sulfuric acid gave sheet resistances of 100 and 141 $\Omega\cdot\square^{-1}$, respectively, the latter value being consistent with that reported by Xia et al.[23] Interestingly, when the sulfuric acid (SA) treatment was carried out following PTSA in DMSO (PD) treatment for one time, the sheet resistance remained ~67 $\Omega\cdot\square^{-1}$ These films had high conductivity of ~3200 $S\cdot cm^{-1}$, coupled with high transparency of 96%, giving a high σ ratio of ~140.

Three SA treatments, following a single PD treatment, further increased conductivity to more than 3300 $S\cdot cm^{-1}$ with transparency of 91%. It must be mentioned that the baking temperature for SA treatment was kept the same as that of PD treatment, so that the effect of PD treatment remained unaltered with respect to temperature.

This shows that, out of all treatments, the joint effect of PTSA and DMSO worked best in decreasing the value of sheet

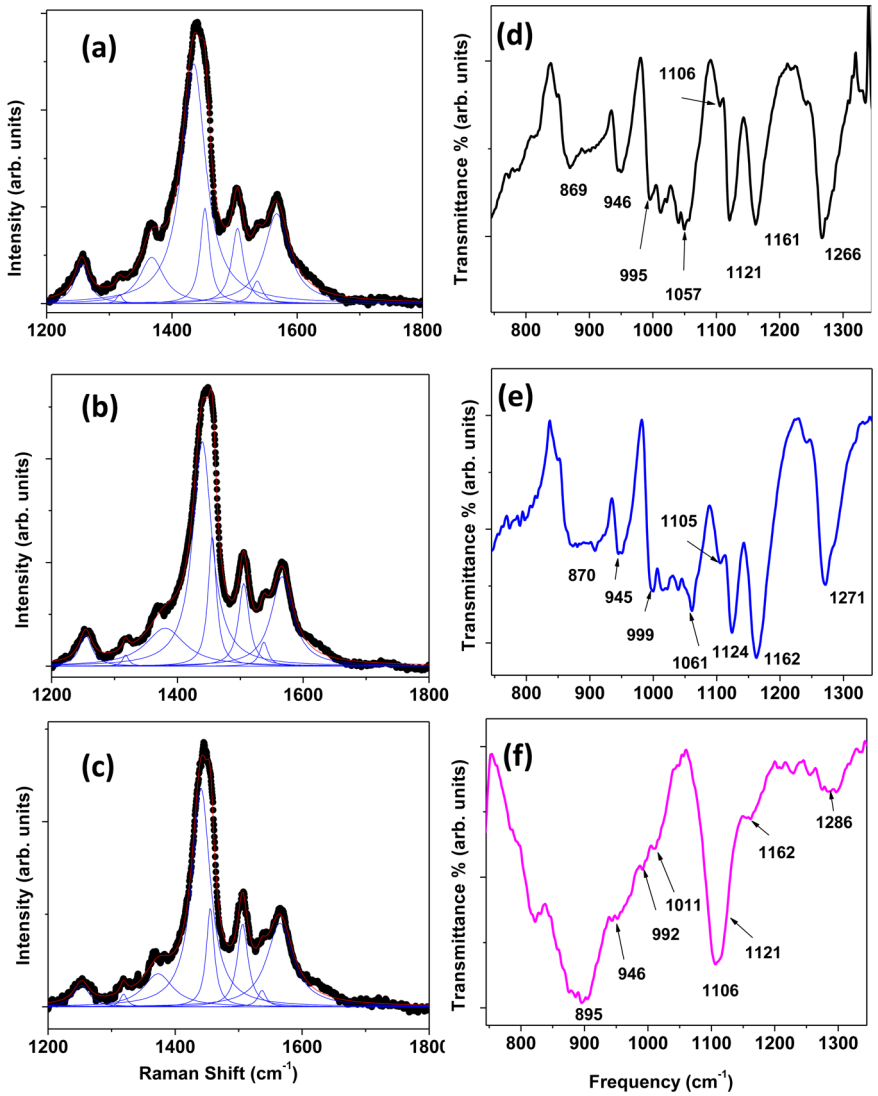

Figure 4. (a–c) Raman and (d–f) FTIR spectra of (a, d) untreated, (b, e) PD, and (c, f) PDSA films.

resistance. Furthermore, additional treatments with either PD or SA yield conductivity values well above 3000 S·cm^{-1}, with σ ratios in the range 70–140. Although the range of σ ratio appears broad, one must remember that a large change in σ ratio corresponds to small changes in transparency. The effect of this change in transparency on device efficiency is probably debatable. For clarity, films treated with PTSA in DMSO are called PDx (x = 1, 2, 3, ..., denoting number of PD treatments). Films treated with additional SA are called PDSAy (y = 1, 2, 3, ..., denoting number of SA treatments). Both types of films were characterized as regards their conductivity, transparency, structure, and morphology, as discussed in the next subsection.

Although most of the results for the PEDOT–PSS films are reported for glass, it must be mentioned that, for some characterizations, films coated on ITO were used. Cross-sectional SEM measurements required the samples to be cut. SEM images for the untreated and treated PEDOT films on glass showed a signs of peeling of the polymer film, probably due to breakage of the films, which led to its surface roughening. This problem was overcome when ITO-coated glass was used as substrate. Hence, SEM measurements were carried out on ITO, for correct estimation of thickness. SEM measurements on ITO showed uniform film coverage, especially for the thin films, as shown in Figure 3c. Also, FTIR and Raman measurements (carried out in reflection modes) of the treated films were conducted on ITO, as the signal obtained was found to improve with ITO than glass, due to better reflectance of the ITO-coated substrate. SIMS was also performed on ITO-coated substrate, to better monitor the interface of the film by use of the indium signal. However, prior to using films on ITO for the different characterizations, the sheet resistance of the PD films on ITO were compared with those on glass (Table S2, Supporting Information). They were found to match fairly well.

As mentioned earlier, all treated films on glass showed good transparency well above 90% at 550 nm (Table S1, Supporting Information), with that of the single layer pristine film being 97%, PD1 and PDSA1 both being 96%, and PD3 having slightly less transparency of 94% (Figure 3a). However, since the R_s value was lowest (~67 Ω·□$^{-1}$) for PD treatment, the value of σ_{DC}/σ_{OP} increased drastically for this film (~127). Additional SA treatment only slightly increased the σ_{DC}/σ_{OP} value to 139, due to slight difference in their %T values (Table S1, Supporting Information). For the other multiple-treated films, it was found that with increase in number of treatments, the R_s value increases, Z decreases, and %T gradually decreases. Thus,

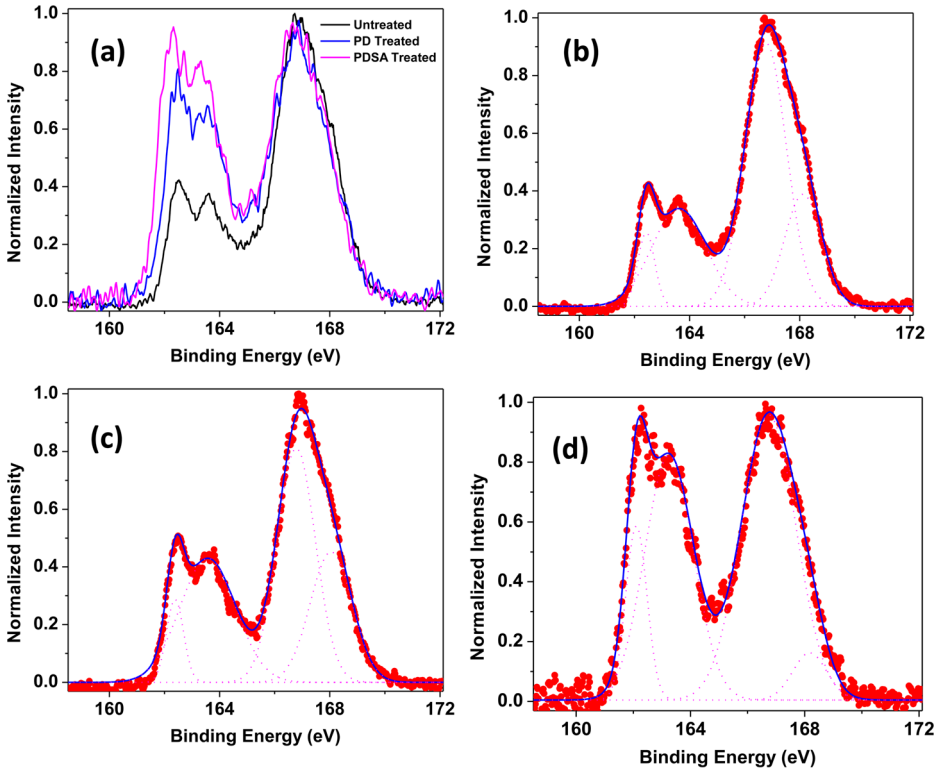

Figure 5. (a) XPS of untreated, PD, and PDSA films, showing the change in S 2p intensity of PEDOT and PSS. Individual fits to data are shown separately for (b) untreated, (c) PD, and (d) PDSA films. Red dots denote experimental data, pink dashed lines denote individual peak fits, and blue bold line denotes composite fit.

the limit to multiple treatment was set such that R_s < 100 $\Omega\cdot\square^{-1}$ and transmittance T > 90%. However, for the PDSAy films, even though all values seemed promising, the film became perforated due to the harsh treatment (Figure 3b) for y > 3.

Posttreatment of the PEDOT−PSS films resulted in change of film thickness as well. A 100 nm PEDOT−PSS film, when treated, gives different thicknesses, depending on the treatment type (Table S1, Supporting Information). PD1, PD3, PD4, and PD5 films had thicknesses of 65, 38, 36, and 30 nm, respectively. PDSA1 and PDSA3 had thicknesses of 48 and 42 nm, respectively. This shows that single PD treatment leads to about ∼35% reduction in film thickness, whereas the additional PD and SA treatments leads to about ∼50% or more reduction in film thickness. As the enhancement of σ_{DC} value depends on reduction of R_s as well as Z, additional PD and SA treatments both give a higher conductivity value well above ∼3000 S·cm^{-1}. It must be mentioned here that although profilometers are routinely used for thickness measurements of this type of films,[23,39] this is a mechanical mean to determine thickness and may induce artifacts in the measurement that underestimate the film thickness. In order to ensure that this was not the case, cross-sectional scanning electron microscopy (SEM) measurements were carried out (Figure 3c) for the films, especially for the lower thickness samples to independently get an estimate of the thickness regime. Results of SEM were found to match well with profilometer measurements.

PD and SA treatments were also carried out on thicker PEDOT−PSS films (Figure S3a, Supporting Information). The R_s values were as low as 20 $\Omega\cdot\square^{-1}$ for the five-layer film with transparency of 60%. The stability of the PD and PDSA films was investigated by exposing them to air under ambient conditions and monitoring the sheet resistance with time, up to 500 h. For this, the films were kept on the bench in covered Petri dishes, without direct exposure to sunlight, and sheet resistance was measured from time to time. The sheet resistance was found to increase by 20% in the first 200 h and remain almost unchanged until 500 h. The rate of increase was found to be comparable to other acid treatments[24] and much less compared to untreated PEDOT−PSS film, which shows an increase of about 45% (Figure S3b, Supporting Information).[24]

Although for this work, PEDOT−PSS films on glass and/or ITO were used, we report our observation that PD films formed uniform coatings on PET sheets as well (Figure S4a, Supporting Information). Unlike films directly treated with sulfuric acid, which were found to completely destroy the PET sheets (Figure S4b, Supporting Information), the PD treatment was found to be very much compatible with flexible organic substrate and moreover, when coated prior to SA treatment, it was effective in shielding the material from the strong effect of sulfuric acid. Since fabrication of TC electrodes on flexible substrates such as PET is an important aspect, we have included our above observation in this regard, in the present paper. Although the films have been tested for sheet resistance (which is found to be consistent with those reported on glass), issues of reproducibility of uniform films with PDSA treatment (as seen in Figure S4b, Supporting Information) and difficulty in carrying out proper thickness measurements for both PD and PDSA films need to be overcome by us, before we provide further quantitative results in this regard.

B. Structural and Morphological Characterization of Films. The PEDOT−PSS films before and after treatments were characterized by Raman and Fourier transform infrared

(FTIR) spectroscopy, along with X-ray photoelectron spectroscopy (XPS), secondary ion mass spectrometry (SIMS), and atomic force microscopy (AFM). Raman spectra of the untreated and treated PEDOT−PSS films, along with their Lorentzian fits, are shown in Figure 4a−c. Although the profiles of the Raman spectra appear to be similar for the treated and untreated films, some interesting information on the change in the doping level is revealed after fitting of the spectra. The central band at 1440 cm^{-1}, corresponding to the symmetric stretch of C_α=C_β mode, is a combination of two bands arising due to the neutral and oxidized structures in PEDOT.[39,40] A change in these bands is related to a change in the degree of doping of PEDOT films.[39−42,48] For the untreated film, the peak corresponding to neutral (oxidized) structure is observed at 1435 (1453) cm^{-1}. Both PD and PDSA films show a considerable blue shift of both these peaks (Table S3, Supporting Information), with the neutral (oxidized) peak at 1440 (1456) cm^{-1}. Moreover, the intensity of the oxidized peak is found to increase compared to the neutral peak for both treated films, with the increase being greater for PD treatment (Table S3, Supporting Information). This increase in intensity of the oxidized peak along with the blue shift of these bands, indicate doping of the films posttreatment.[41,42]

FTIR spectroscopy (Figure 4d−f) was carried out for untreated, PD, and PDSA films. The bands from 800 to 1100 cm^{-1} are mainly associated with PEDOT structure, and the bands above 1100 cm^{-1} are attributed to PSS structure.[49−51] The peaks at 1266 and 1161 cm^{-1} for untreated PEDOT−PSS film are attributed to asymmetric and symmetric vibrations of SO_3 groups in PSS chains, respectively.[51] For the PD film (Figure 4e), both these peaks are present with the asymmetric (symmetric) stretch observed at 1271 (1162) cm^{-1}. The 5 cm^{-1} peak shift of the asymmetric SO_3 stretch mode probably indicates different interaction of PEDOT with the SO_3 groups in the PD film compared to the untreated film, which may be due to phase separation of PSS and/or incorporation of SO_3 from PTSA. However, for the PDSA film (Figure 4f), the asymmetric (symmetric) SO_3 stretches, observed at 1286 (1162) cm^{-1}, show drastic reduction indicating decrease in SO_3 group intensity, a signature of PSS as well as PTSA removal from the system due to the additional SA treatment. This is consistent with sulfuric acid treatment reported by Xia et al.[23] Moreover, when the FTIR spectra of untreated and PD/PDSA films are compared, it is observed that the PEDOT structure remains more or less unaffected by PD treatment, whereas it changes drastically due to additional SA treatment. This indicates that the two dopant acids, PTSA and SA, have very different effect on PEDOT−PSS structure and thus on its conductivity enhancement mechanism. The Raman and FTIR results do not point to any conformational change in PEDOT, as observed in some posttreatments.[52]

In order to ascertain whether PD treatment causes removal of PSS from the PEDOT−PSS film, XPS was carried out on untreated and treated films (Figure 5). XPS bands between 166 and 172 eV are the S 2p band of sulfur atoms in PSS, whereas those between 162 and 166 eV are the S 2p band of sulfur atoms in PEDOT.[23,25] As shown in Figure 5a, the intensity ratio of PEDOT to PSS saliently increased for both PD and PDSA films compared to the untreated film, being greater for PDSA. Individual XPS spectra for the films were fit by Gaussian function (Figure 5b−d). The parameters of fit versus peak position (x), peak width (w), and area under the individual peaks (A') are shown in Table S4 in Supporting Information. As seen from this table, for the untreated film (Figure 5b), the two peaks at 162.4 and 163.6 eV correspond to S $2p_{3/2}$ and S $2p_{1/2}$ sulfur signals from PEDOT, whereas the two peaks at 166.8 and 168.2 eV correspond to S $2p_{3/2}$ and S $2p_{1/2}$ sulfur signal from PSS. The sum (A) of the individual area under the peaks (A') corresponding to S $2p_{3/2}$ and S $2p_{1/2}$ sulfur signals of PEDOT (PSS) gives the intensity of the S 2p band of PEDOT (PSS), denoted by $A^{S2p}{}_{PEDOT}$ ($A^{S2p}{}_{PSS}$). The S 2p intensity ratio of PEDOT to PSS ($A^{S2p}{}_{PEDOT}$:$A^{S2p}{}_{PSS}$) was calculated, and the values are given in Table S4 in Supporting Information. The ratio was found to decrease from 1:2.39 for the untreated film to 1:1.31 (1:0.56) for the PD (PDSA) treated films. A decrease in the $A^{S2p}{}_{PEDOT}$:$A^{S2p}{}_{PSS}$ ratio upon treatment typically indicated the removal of some PSSH chains from the PEDOT−PSS film.[23,25] However, for multiple PD treatment (Figure S5 in Supporting Information), we found that the S 2p ratio slightly decreased for PD3 and PD5 compared to PD1, in the order PD3 < PD5 < PD1. We believe that, due to PD treatment, there is incorporation of SO_3 groups from PTSA, along with removal of the same from PSS in the film. The SO_3 groups from PTSA have the same chemical environment as those of PSS and thus contributed to the same S 2p peak intensity. Thus, in the case of PD films, the S 2p intensity ratio is affected by the competing process of addition and removal of SO_3 groups, which varies for each treatment. However, all values for the treated films were greater compared to the untreated film. This, along with the observed shift of SO_3 groups in the PD film from its FTIR spectra and the decrease in film thickness with successive PD treatment, suggest that PD treatment not only phase-separates PSS from PEDOT and removes the former as PSSH but also incorporates SO_3 groups from PTSA. This removal of PSSH is in accordance with the decrease in thickness of the film, along with negligible change in sheet resistance or transparency of the films.

An additional SIMS depth profiling of PD films was carried out to investigate whether PSS removal was occurring throughout the depth of the PD films. It must be mentioned that due to PSS removal and/or SO_3 addition from PTSA, the sulfur/carbon (S/C) elemental ratio of the treated films may change. For PSS removal to have occurred throughout the film, this changed ratio should, however, remain fairly unaltered over the entire film depth. This was checked by monitoring the variation of S/C intensity ratio as a function of sample depth by SIMS. For this, sulfur (Figure 6) and carbon (Figure 6, inset I) secondary ion signals were individually monitored as a function of sputter time for PD3 and PD5 films, at a constant sputter rate of 0.5 $Å{\cdot}s^{-1}$. Both intensities were observed to be $>10^5$ counts per second (cps) for the first part of the profile (i.e., for the signal from the films), during which both were found to remain almost unaltered, indicating fair in-depth elemental homogeneity of the films. After this, a sharp fall in both signals was observed, demarking the film/substrate interface. From the individual sulfur and carbon intensities, the S/C secondary ion intensity ratio was calculated for the PD3 and PD5 films (Figure 6, inset II). These were found to remain fairly constant throughout the film depth for both films.

Atomic force microscopy (Figure 7) was carried out in tapping mode to elucidate the morphology of the posttreated films. AFM topographic images of untreated, PD, and PDSA films showed signature changes in morphology of the films upon posttreatment. Unlike the untreated film, which does not show prominent grains, both PD and PDSA films show spherical-shaped particles, with the size of grains being larger

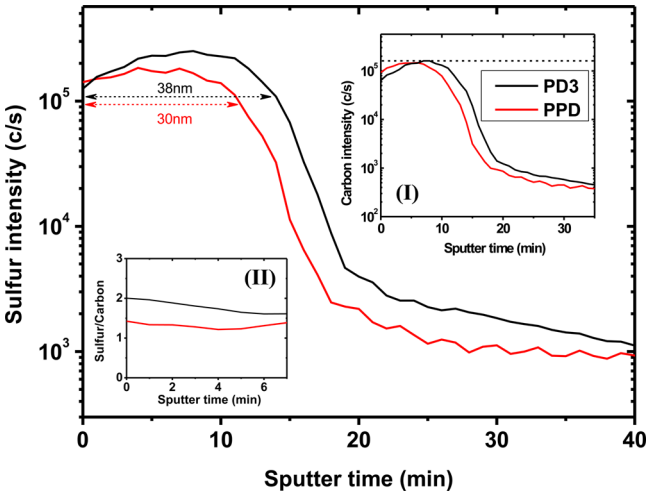

Figure 6. SIMS depth profiling of PD films showing variation of sulfur, carbon, and sulfur/carbon intensity with sputter time.

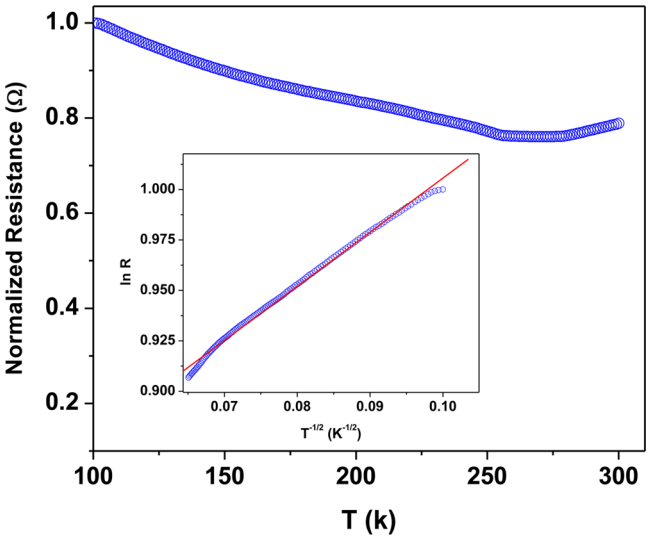

Figure 8. Normalized resistance vs temperature with a plot of ln R vs $T^{-1/2}$ (inset) for the PD film.

for PD film and much smaller for PDSA film. This morphological change is similar to the treatment of PEDOT−PSS films by oxalic, malonic, and methanesulfonic acid[25] but different from that of direct treatment with sulfuric acid.[23]

C. Low-Temperature Resistivity Measurements. The temperature dependence of resistance, measured in a four-probe configuration, of the PD-treated PEDOT−PSS film was investigated from 300 down to 100 K (Figure 8). Below 250 K, the resistance of the PD film was found to decrease with increasing temperature. It became almost constant at temperatures above 255 K, suggesting semimetallic behavior.[23,25,53] Temperature (T) dependence of the resistance (R) (Figure 8 inset) was found to obey the one-dimensional variable range hopping (VRH) model, given by[54,55]

$$R(T) \propto \exp(T_0/T)^{1/2} \quad (3)$$

where T_0 is the energy barrier between localized states, related to the density of states at the Fermi level.[23] The plot of ln R versus $T^{-1/2}$ showed a linear relationship in the low-temperature range below 220 K. The plot deviated from the linear relationship at $T > 220$ K. T_0 value estimated from the linear relationship was 7.2 K. This behavior of the PD-treated PEDOT−PSS film was found to be saliently different from that of the untreated PEDOT−PSS film.[23] The latter is reported to have a linear ln R versus $T^{-1/2}$ relationship in the whole temperature range from 110 to 300 K, with T_0 values that are orders of magnitude higher. The difference in behavior of the PD-treated film with respect to the untreated film is at par with PEDOT−PSS films treated with other acids, which are reported to obey same one-dimensional hopping model.[23,25] Thus, like other reported acids, PD treatment of PEDOT−PSS is observed to cause significant reduction in the energy barrier for interchain and interdomain charge hopping. The difference between PEDOT−PSS and a highly conducting PEDOT−Tos have also been discussed by Bubnova et al.[53] in the context of semimetallic polymers. They have shown that PEDOT−PSS is a Fermi glass but PEDOT−Tos (from spin-coating and VPP) is a semimetal.[53]

D. Application of PD Films in Transparent Conductive Oxide- and Platinum-Free Counter Electrode for Dye-Sensitized Solar Cells. To demonstrate the application of the highly conducting PD films as suitable replacements to inorganic TCs, the material was used as a counter electrode, free of platinum and FTO, in a dye-sensitized solar cell (DSSC). In a standard DSSC, the counter electrode is an inorganic transparent conductive oxide (TCO), platinized to render it highly catalytic toward I^-/I_3^-redox couple, as inorganic TCs alone have no appreciable catalytic activity toward I^-/I_3^-redox couple. PEDOT has been reported to show good electrocatalytic activity for various electrochemical conversions, such as oxygen reduction[56,57] and proton reduction,[58] and thus is a potential electrode in fuel cell technology. PEDOT is a potential candidate for the replacement of platinum and TCO on counter electrode in DSSC due to its high conductivity and good catalytic activity toward I^-/I_3^- redox couple.[59,60] It has already been reported

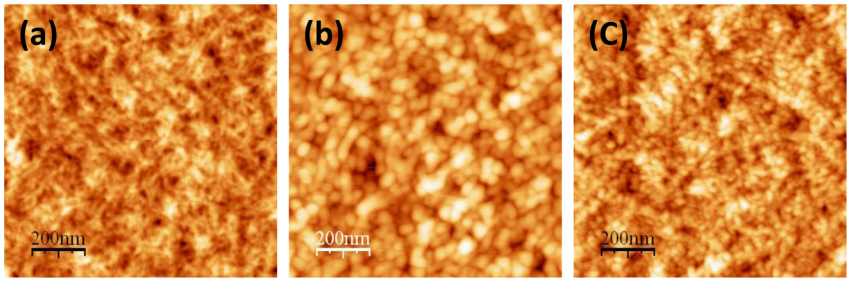

Figure 7. AFM topographic images (1 × 1 μm^2) of (a) untreated, (b) PD, and (c) PDSA films.

dx.doi.org/10.1021/am504150n | ACS Appl. Mater. Interfaces 2014, 6, 17792−17803

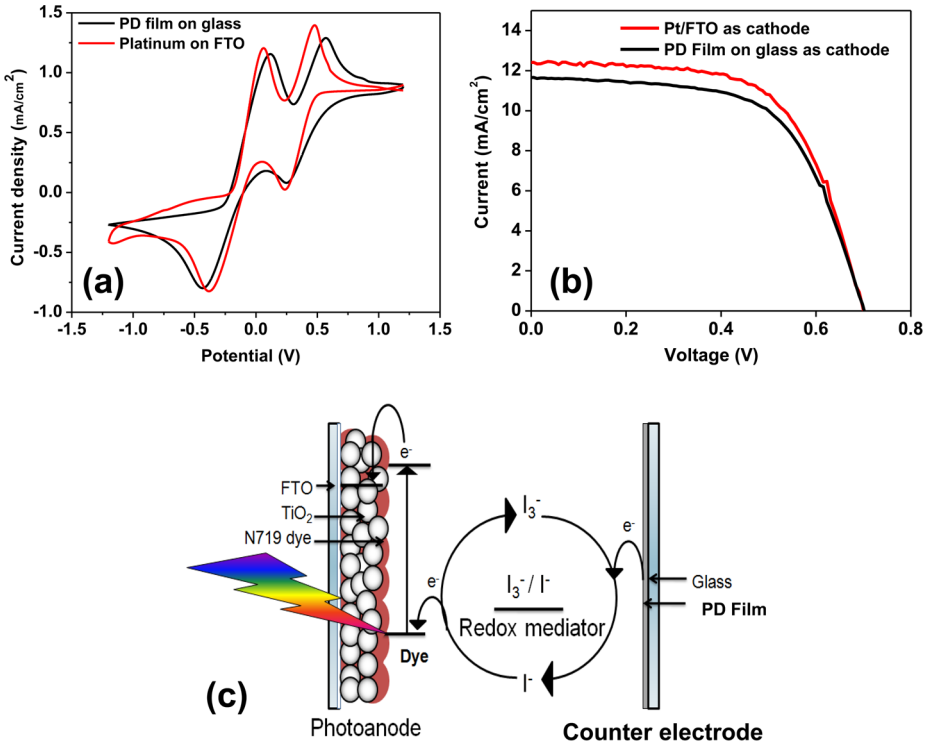

Figure 9. (a) Cyclic voltammogram of PD films on glass (black) and sputtered Pt on FTO (red) in acetonitrile solution of 10 mM LiI, 1 mM I_2, and 0.1 M $LiClO_4$ at a scan rate of 20 mV/s. (b) Current vs voltage curves of DSSCs using the standard Pt/FTO (red) and PD film on glass (black) as counter electrode. (c) Schematic representation of DSSC based on PD film as counter electrode.

that electropolymerized PEDOT[61−63] has similar catalytic activity to platinum, but since it has lower conductivity a conductive layer is required below it, which might be either TCO or any other conducting PEDOT layer. Previously reported PEDOT-based counter electrodes were made up of either in situ polymerized PEDOT films,[60,64] electropolymerized PEDOT,[61−63] or PEDOT−PSS blended with some conducting materials such as graphene and carbon nanotubes (CNT)[65,66] on top of either TCO or conducting PEDOT−PSS. As per our information, there is no report to date which shows that PEDOT−PSS, after appropriate secondary treatment, alone can act as both conducting and catalytic for I^-/I_3^-redox couple in DSSC. Interestingly, we found these PD films have promising catalytic behavior for reducing I_3^- to I^-. The cyclic voltammogram (Figure 9a) shows that the PD film has catalytic activity comparable to that of Pt/FTO. The DSSC with PD film was fabricated (schematic shown in Figure 9c) and compared with a standard Pt/FTO-based cell. A picture of the fabricated DSSC based on PD film is given in Figure S6 of Supporting Information. $J-V$ characteristics (Figure 9b) of the same showed power conversion efficiency (PCE) of 5.00%, accompanied by short-circuit current density (J_{sc}) of 11.62 mA·cm^{-2}, open-circuit voltage (V_{oc}) of 714 mV, and fill factor (FF) of 0.60. All values are comparable to those obtained for the standard Pt/FTO counter electrode (Table S5 of Supporting Information). Thus, on the basis of cyclic voltammetry and DSSC device results, we believe that the PD films do have potential to replace Pt, as we obtained almost equal efficiency of the DSSC with PD films replacing the highly reflecting Pt electrode.

IV. CONCLUSION

In this work, the posttreatment of PEDOT−PSS thin films by a combination of *p*-toluenesulfonic acid, dimethyl sulfoxide, and sulfuric acid was investigated. Results showed a significant increase in both electrical conductivity (σ_{DC}) and the figure of merit (σ_{DC}/σ_{OP}) of PEDOT−PSS films. A multitechnique approach was taken to elucidate information regarding film structure. Combined results of Raman, FTIR, XPS, and SIMS indicated that conductivity enhancement was due to doping, rearrangement of PEDOT particles owing to phase separation, and removal of PSS matrix throughout the depth of the film, along with incorporation of SO_3 groups from PTSA. The temperature dependence of resistance for the treated films was found to be in accordance with one-dimensional variable range hopping, showing that treatment is effective in reducing energy barriers for interchain and interdomain charge hopping. The increase in conductivity of films was found to be associated with a change in film morphology, which indicated phase separation of PSS from PEDOT nanoparticles. The treatment was found to be compatible with both glass and PET substrates. Apart from being a promising material for photovoltaic applications, the films exhibited potential catalytic activity as well and successfully replaced platinum and fluorinated tin oxide as counter electrode in dye-sensitized solar cells.

■ ASSOCIATED CONTENT

Supporting Information

Six figures and five tables showing variation of conductivity and σ ratio; thickness calibration of spin coater; values of conductivity, transparency, and σ ratio of treated films; comparison of sheet resistance of PD films on ITO and glass; variation of sheet resistance with number of layers in PEDOT−PSS films and stability check for treated film; PD films on PET;

Raman data; XPS data analysis; XPS spectra of multiple treated PD films; picture of fabricated DSSC; and DSSC device parameters. This material is available free of charge via the Internet at http://pubs.acs.org.

AUTHOR INFORMATION

Corresponding Author

*E-mail anilkumar@iitb.ac.in; phone +91 22-2576 7153; fax +91 22-2576 7152.

Present Address

[⊥]Institut des Nanosciences de Paris, 4 Place Jussieu, Paris, France.

Author Contributions

The manuscript was written through contributions of all authors. All authors have given approval to the final version of the manuscript.

Funding

This work was supported by DIT and MNRE projects.

Notes

The authors declare no competing financial interest.

ACKNOWLEDGMENTS

S.M. thanks Professor C. V. Tomy for his help with LTR measurement facility and Professors K.L. Narasimhan and D. Kabra for fruitful discussions. All central facilities of IIT Bombay (Raman, SIMS facilities at SAIF, XPS, FTIR, UV−vis at CEN, and SPM at IRCC) are acknowledged. We acknowledge Department of Electronics and Information Technology and Ministry of New and Renewable Energy, India, for financial support. S.M. thanks the DIT project for a postdoctoral research grant. S.G. thanks NCPRE aided by MNRE, Government of India, for a research fellowship.

ABBREVIATIONS

PEDOT−PSS, poly(3,4-ethylenedioxythiophene)−polystyrenesulfonate
TC, transparent conductor
PET, poly(ethylene terephthalate)
ITO, indium tin oxide
FTO, fluorine-doped tin oxide
PTSA, *p*-toluenesulfonic acid
DMSO, dimethyl sulfoxide
SA, sulfuric acid
PD, *p*-toluenesulfonic acid in dimethyl sulfoxide
PDSA, *p*-toluenesulfonic acid in dimethyl sulfoxide, followed by sulfuric acid
FTIR, Fourier transform infrared
SEM, scanning electron microscopy
XPS, X-ray photoelectron spectroscopy
TOF-SIMS, time-of-flight secondary ion mass spectrometry
AFM, atomic force microscopy
LTR, low-temperature resistivity
VRH, variable range hopping
DSSC, dye-sensitized solar cell
PCE, power conversion efficiency

REFERENCES

(1) Inganas, O. Organic Photovoltaics: Avoiding Indium. *Nat. Photonics* **2011**, *5*, 201−202.

(2) Sondergaard, R.; Hosel, M.; Angmo, D.; Larsen-Olsen, T. T.; Krebs, F. C. Roll-to-Roll Fabrication of Polymer Solar Cells. *Mater. Today* **2012**, *15*, 36−49.

(3) Han, T.-H.; Lee, Y.; Choi, M.-R.; Woo, S.-H.; Bae, S.-H.; Hong, B. H.; Ahn, J.-H.; Lee, T.-W. Extremely Efficient Flexible Organic Light-Emitting Diodes with Modified Graphene Anode. *Nat. Photonics* **2012**, *6*, 105−110.

(4) Chen, T. L.; Ghosh, D. S.; Krautz, D.; Cheylan, S.; Pruneri, V. Highly Stable Al-Doped ZnO Transparent Conductors Using an Oxidized Ultrathin Metal Capping Layer at its Percolation Thickness. *Appl. Phys. Lett.* **2011**, *99*, No. 093302.

(5) Guzman, G.; Dahmani, B.; Puetz, J.; Aegerter, M. A. Transparent Conducting Sol−Gel ITO Coatings for Display Applications by an Improved Dip Coating Technique. *Thin Solid Films* **2006**, *502*, 281−285.

(6) Zhu, R.; Chung, C.-H.; Cha, K. C.; Yang, W.; Zheng, Y. B.; Zhou, H.; Song, T.-B.; Chen, C.-C.; Weiss, P. S.; Li, G.; Yang, Y. Fused Silver Nanowires with Metal Oxide Nanoparticles and Organic Polymers for Highly Transparent Conductors. *ACS Nano* **2011**, *5*, 9877−9882.

(7) Lee, J.-Y.; Connor, S. T.; Cui, Y.; Peumans, P. Solution-Processed Metal Nanowire Mesh Transparent Electrodes. *Nano Lett.* **2008**, *8*, 689−692.

(8) Tu, K.-H.; Li, S.-S.; Li, W.-C.; Wang, D.-Y.; Yang, J.-R.; Chen, C.-W. Solution Processable Nanocarbon Platform for Polymer Solar Cell. *Energy Environ. Sci.* **2011**, *4*, 3521−3526.

(9) Wu, Z.; Chen, Z.; Du, X.; Logan, J. M.; Sippel, J.; Nikolou, M.; Kamaras, K.; Reynolds, J. R.; Tanner, D. B.; Hebard, A. F.; Rinzler, A. G. Transparent, Conductive Carbon Nanotube Films. *Science* **2004**, *305*, 1273−1276.

(10) Gruner, G. J. Carbon Nanotube Films for Transparent and Plastic Electronics. *J. Mater. Chem.* **2006**, *16*, 3533−3539.

(11) Gomez De Arco, L.; Zhang, Y.; Schlenker, C. W.; Ryu, K.; Thompson, M. E.; Zhou, C. Continuous, Highly Flexible, and Transparent Graphene Films by Chemical Vapor Deposition for Organic Photovoltaics. *ACS Nano* **2010**, *4*, 2865−2873.

(12) Bae, S.; Kim, H.; Lee, Y.; Xu, X.; Park, J.-S.; Zheng, Y.; Balakrishnan, J.; Lei, T.; Kim, H. R.; Song, Y. I.; Kim, Y.-J.; Kim, K. S.; Özyilmaz, B.; Ahn, J.-H.; Hong, B. H.; Iijima, S. Roll-to-Roll Production of 30-Inch Graphene Films for Transparent Electrodes. *Nat. Nanotechnol.* **2010**, *5*, 574−578.

(13) Gustafsson, G.; Cao, Y.; Treacy, G. M.; Klavetter, F.; Colaneri, N.; Heeger, A. J. Flexible Light-Emitting Diodes Made from Soluble Conducting Polymers. *Nature* **1992**, *357*, 477−479.

(14) Zhang, F.; Johansson, M.; Andersson, M. R.; Hummelen, J. C.; Inganas, O. Polymer Photovoltaic Cells with Conducting Polymer Anodes. *Adv. Mater.* **2002**, *14*, 662−665.

(15) Xia, Y.; Sun, K.; Ouyang, J. Highly Conductive Poly(3,4-ethylenedioxythiophene):Poly(styrene sulfonate) Films Treated with an Amphiphilic Fluoro Compound as the Transparent Electrode of Polymer Solar Cells. *Energy Environ. Sci.* **2012**, *5*, 5325−5332.

(16) Ouyang, J.; Chu, C. W.; Chen, F. C.; Xu, Q.; Yang, Y. Highly Conductive PEDOT:PSS Film and its Applications in Optoelectronic Devices. *Adv. Funct. Mater.* **2005**, *15*, 203−208.

(17) Wang, P.-C.; Liu, L.-H.; Mengistie, D. A.; Li, K.-H.; Wen, B.-J.; Liu, T.-S.; Chu, C.-W. Transparent Electrodes Based on Conducting Polymers for Display Applications. *Displays* **2013**, *34*, 301−314.

(18) Friend, R. H.; Gymer, R. W.; Holmes, A. B.; Burroughes, J. H.; Marks, R. N.; Taliani, C.; Bradley, D. D. C.; Santos, D. A. D.; Brédas, J. L.; Lögdlund, M.; Salaneck, W. R. Electroluminescence in Conjugated Polymers. *Nature* **1999**, *397*, 121−128.

(19) Groenendaal, L.; Jonas, F.; Freitag, D.; Pielartzik, H.; Reynolds, J. R. Poly(3,4-ethylenedioxythiophene) and its Derivatives: Past, Present, and Future. *Adv. Mater.* **2000**, *12*, 481−494.

(20) Ouyang, J. "Secondary Doping" Methods to Significantly Enhance the Conductivity of PEDOT:PSS for Its Application as Transparent Electrode of Optoelectronic Devices. *Displays* **2013**, *34*, 423−436.

(21) Vosgueritchian, M.; Lipomi, D. J.; Bao, Z. Highly Conductive and Transparent PEDOT:PSS Films with a Fluorosurfactant for Stretchable and Flexible Transparent Electrodes. *Adv. Funct. Mater.* **2012**, *22*, 421−428.

(22) Commercially available under trade name "Clevios-PH1000" (http://www.heraeus-clevios.com/en/products/heraeus-conductive-polymers-products.aspx).
(23) Xia, Y.; Sun, K.; Ouyang, J. Solution-Processed Metallic Conducting Polymer Films as Transparent Electrode of Optoelectronic Device. *Adv. Mater.* **2012**, *24*, 2436−2440.
(24) Mengistie, D. A.; Ibrahem, M. A.; Wang, P.-C.; Chu, C.-W. Highly Conductive PEDOT:PSS Treated with Formic Acid for ITO-Free Polymer Solar Cells. *ACS Appl. Mater. Interfaces* **2014**, *6*, 2292−2299.
(25) Ouyang, J. Solution-Processed PEDOT:PSS Films with Conductivities as Indium Tin Oxide through a Treatment with Mild and Weak Organic Acids. *ACS Appl. Mater. Interfaces* **2013**, *5*, 13082−13088.
(26) Nardes, A. M.; Kemerink, M.; De Kok, M. M.; Vinken, E.; Maturova, K.; Janssen, R. A. J. Conductivity, Work Function, and Environmental Stability of PEDOT:PSS Thin Films Treated with Sorbitol. *Org. Electron.* **2008**, *9*, 727−734.
(27) Kim, Y. H.; Sachse, C.; Machala, M. L.; May, C.; Muller-Meskamp, L.; Leo, K. Highly Conductive PEDOT:PSS Electrode with Optimized Solvent and Thermal Post-Treatment for ITO-Free Organic Solar Cells. *Adv. Funct. Mater.* **2011**, *21*, 1076−1081.
(28) Alemu, D.; Wei, H.-Y.; Ho, K.-C.; Chu, C.-W. Highly Conductive PEDOT:PSS Electrode by Simple Film Treatment with Methanol for ITO-Free Polymer Solar Cells. *Energy Environ. Sci.* **2012**, *5*, 9662−9671.
(29) Xia, Y.; Ouyang, J. Anion Effect on Salt-Induced Conductivity Enhancement of Poly(3,4-ethylenedioxythiophene):Poly(styrenesulfonate) Films. *Org. Electron.* **2010**, *11*, 1129−1135.
(30) Xia, Y.; Ouyang, J. Significant Conductivity Enhancement of Conductive Poly(3,4-ethylenedioxythiophene):Poly(styrenesulfonate) Films through a Treatment with Organic Carboxylic Acids and Inorganic Acids. *ACS Appl. Mater. Interfaces* **2010**, *2*, 474−483.
(31) Xia, Y.; Zhang, H.; Ouyang, J. Highly Conductive PEDOT:PSS Films Prepared through a Treatment with Zwitterions and Their Application in Polymer Photovoltaic Cells. *J. Mater. Chem.* **2010**, *20*, 9740−9747.
(32) Xia, Y.; Ouyang, J. PEDOT:PSS Films with Significantly Enhanced Conductivities Induced by Preferential Solvation with Cosolvents and Their Application in Polymer Photovoltaic Cells. *J. Mater. Chem.* **2011**, *21*, 4927−4936.
(33) Badre, C.; Marquant, L.; Alsayed, A. M.; Hough, L. A. Highly Conductive Poly(3,4-ethylenedioxythiophene):Poly(styrenesulfonate) Films Using 1-Ethyl-3-Methylimidazolium Tetracyanoborate Ionic Liquid. *Adv. Funct. Mater.* **2012**, *22*, 2723−2727.
(34) De, S.; Higgins, T. M.; Lyons, P. E.; Doherty, E. M.; Nirmalraj, P. N.; Blau, W. J.; Boland, J. J.; Coleman, J. N. Silver Nanowire Networks as Flexible, Transparent, Conducting Films: Extremely High DC to Optical Conductivity Ratios. *ACS Nano* **2009**, *3*, 1767−1774.
(35) De, S.; Coleman, J. N. Are There Fundamental Limitations on the Sheet Resistance and Transmittance of Thin Graphene Films? *ACS Nano* **2010**, *4*, 2713−2720.
(36) Scardaci, V.; Coull, R.; Coleman, J. N. Very Thin Transparent, Conductive Carbon Nanotube Films on Flexible Substrates. *Appl. Phys. Lett.* **2010**, *97*, No. 023114.
(37) Hojati-Talemi, P.; Bächler, C.; Fabretto, M.; Murphy, P.; Evans, D. Ultrathin Polymer Films for Transparent Electrode Applications Prepared by Controlled Nucleation. *ACS Appl. Mater. Interfaces* **2013**, *5*, 11654−11660.
(38) Kim, N.; Kee, S.; Lee, S. H.; Lee, B. H.; Kahng, Y. H.; Jo, Y.-R.; Kim, B.-J.; Lee, K. Highly Conductive PEDOT:PSS Nanofibrils Induced by Solution-Processed Crystallization. *Adv. Mater.* **2014**, *26*, 2268−2272.
(39) Reyes-Reyes, M.; Cruz-Cruz, I.; López-Sandoval, R. Enhancement of the Electrical Conductivity in PEDOT:PSS Films by the Addition of Dimethyl Sulfate. *J. Phys. Chem. C* **2010**, *114*, 20220−20224.
(40) Luo, J.; Luo, J.; Billep, D.; Waechtler, T.; Otto, T.; Toader, M.; Gordan, O.; Sheremet, E.; Martin, J.; Hietschold, M.; Zahn, D. R. T.; Gessner, T. Enhancement of the Thermoelectric Properties of PEDOT:PSS Thin Films by Post-Treatment. *J. Mater. Chem. A* **2013**, *1*, 7576−7583.
(41) Zhang, T.-L.; Chen, H.-Y.; Su, C.-Y.; Kuang, D.-B. A Novel TCO- and Pt-Free Counter Electrode for High Efficiency Dye-Sensitized Solar Cells. *J. Mater. Chem. A* **2013**, *1*, 1724−1730.
(42) Mengistie, D. A.; Wang, P. C.; Chu, C. W. Effect of Molecular Weight of Additives on the Conductivity of PEDOT:PSS and Efficiency for ITO-Free Organic Solar Cells. *J. Mater. Chem. A* **2013**, *1*, 9907−9915.
(43) Fabretto, M. V.; Evans, D. R.; Mueller, M.; Zuber, K.; Hojati-Talemi, P.; Short, R. D.; Wallace, G. G.; Murphy, P. J. Polymeric Material with Metal-Like Conductivity for Next Generation Organic Electronic Devices. *Chem. Mater.* **2012**, *24*, 3998−4003.
(44) Brooke, R.; Evans, D.; Dienel, M.; Hojati-Talemi, P.; Murphy, P.; Fabretto, M. Inkjet Printing and Vapor Phase Polymerization: Patterned Conductive PEDOT for Electronic Applications. *J. Mater. Chem. C* **2013**, *1*, 3353−3358.
(45) Yuk, J. M.; Lee, J. Y.; Kim, Y.; No, Y. S.; Kim, T. W.; Choi, W. K. Formation Mechanisms of Metallic Zn Nanodots by Using ZnO Thin Films Deposited on *n*-Si Substrates. *Appl. Phys. Lett.* **2010**, *97*, No. 061901.
(46) Lee, S. H.; Park, H.; Kim, S.; Son, W.; Cheong, I. W.; Kim, J. H. Transparent and Flexible Organic Semiconductor Nanofilms with Enhanced Thermoelectric Efficiency. *J. Mater. Chem. A* **2014**, *2*, 7288−7294.
(47) Mathew, A.; Rao, G. M.; Munichandriah, N. Effect of TiO_2 Electrode Thickness on Photovoltaic Properties of Dye Sensitized Solar Cell Based on Randomly Oriented Titania. Nanotubes. *Mater. Chem. Phys.* **2011**, *127*, 95−101.
(48) Farah, A. A.; Rutledge, S. A.; Schaarschmidt, A.; Lai, R.; Freedman, J. P.; Helmy, A. S. Conductivity Enhancement of Poly(3,4-ethylenedioxythiophene)-Poly(styrenesulfonate) Films Post-Spincasting. *J. Appl. Phys.* **2012**, *112*, No. 113709.
(49) Selvaganesh, S. V.; Mathiyarasu, J.; Phani, K. L. N.; Yegnaraman, V. Chemical Synthesis of PEDOT−Au Nanocomposite. *Nanoscale Res. Lett.* **2007**, *2*, 546−549.
(50) Nagarajan, S.; Kumar, J.; Bruno, F. F.; Samuelson, L. A.; Nagarajan, R. Biocatalytically Synthesized Poly(3,4-ethylenedioxythiophene). *Macromolecules* **2008**, *41*, 3049−3052.
(51) Jian, J.; Guoa, X.; Lin, L.; Cai, Q.; Cheng, J.; Li, J. Gas-Sensing Characteristics of Dielectrophoretically Assembled Composite Film of Oxygen Plasma-Treated SCNTs and PEDOT/PSS Polymer. *Sens. Actuators, B* **2013**, *178*, 279−288.
(52) Ouyang, J.; Xua, Q.; Chua, C.-W.; Yanga, Y.; Lib, G.; Shinar, J. On the Mechanism of Conductivity Enhancement in Poly(3,4-ethylenedioxythiophene):Poly(styrene sulfonate) Film through Solvent Treatment. *Polymer* **2004**, *45*, 8443−8450.
(53) Bubnova, O.; Khan, Z. U.; Wang, H.; Braun, S.; Evans, D. R.; Fabretto, M.; Hojati-Talemi, P.; Dagnelund, D.; Arlin, J.-B.; Geerts, Y. H.; Desbief, S.; Breiby, D. W.; Andreasen, J. W.; Lazzaroni, R.; Chen, W. M.; Zozoulenko, I.; Fahlman, M.; Murphy, P. J.; Berggren, M.; Crispin, X. Semi-Metallic Polymers. *Nat. Mater.* **2014**, *13*, 190−194.
(54) Kim, J. Y.; Jung, J. H.; Lee, D. E.; Joo, J. Enhancement of Electrical Conductivity of Poly(3,4-ethylenedioxythiophene)/Poly(4-styrenesulfonate) by a Change of Solvents. *Synth. Met.* **2002**, *126*, 311−316.
(55) Joo, J.; Long, S. M.; Pouget, J. P.; Oh, E. J.; Macdiarmid, A. G.; Epstein, A. J. Charge Transport of the Mesoscopic Metallic State in Partially Crystalline Polyanilines. *Phys. Rev. B* **1998**, *57*, 9567−9580.
(56) Winther-Jensen, B.; Winther-Jensen, O.; Forsyth, M.; MacFarlane, D. R. High Rates of Oxygen Reduction over a Vapor Phase-Polymerized PEDOT Electrode. *Science* **2008**, *321*, 671−674.
(57) Cottis, P. P.; Evans, D.; Fabretto, M.; Pering, S.; Murphy, P.; Hojati-Talemi, P. Metal-Free Oxygen Reduction Electrodes Based on Thin PEDOT Films with High Electrocatalytic Activity. *RSC Adv.* **2014**, *4*, 9819−9824.

(58) Winther-Jensen, B.; Fraser, K.; Ong, C.; Forsyth, M.; MacFarlane, D. R. Conducting Polymer Composite Materials for Hydrogen Generation. *Adv. Mater.* **2010**, *22*, 1727−1730.
(59) Zhang, T. L.; Chen, H. Y.; Su, C. Y.; Kuang, D. B. A Novel TCO- and Pt-Free Counter Electrode for High Efficiency Dye-Sensitized Solar Cells. *J. Mater. Chem. A* **2013**, *1*, 1724−1730.
(60) Lee, K. S.; Lee, H. K.; Wang, D. H.; Park, N. G.; Lee, J. Y.; Park, O. O.; Park, J. H. Dye-Sensitized Solar Cells with Pt- And TCO-Free Counter Electrodes. *Chem. Commun.* **2010**, *46*, 4505−4507.
(61) Trevisan, R.; Döbbelin, M.; Boix, P. P.; Barea, E. M.; Zaera, R. T.; Seró, I. M.; Bi□uert, J. PEDOT Nanotube Arrays as High Performing Counter Electrodes for Dye Sensitized Solar Cells: Study of the Interactions Among Electrolytes and Counter Electrodes. *Adv. Energy Mater.* **2011**, *1*, 781−784.
(62) Xiao, Y. M.; Lin, J. Y.; Wu, J. H.; Tai, S. Y.; Yue, G. T. Pulse Potentiostatic Electropolymerization of High Performance PEDOT Counter Electrodes for Pt-Free Dye-Sensitized Solar Cells. *Electrochim. Acta* **2012**, *83*, 221−226.
(63) Kung, C. W.; Cheng, Y. H.; Chen, H. W.; Vittal, R.; Ho, K. C. Hollow Microflower Arrays of PEDOT and Their Application for the Counter Electrode of a Dye-Sensitized Solar Cell. *J. Mater. Chem. A* **2013**, *1*, 10693−10702.
(64) Kwon, J.; Ganapathy, V.; Kim, Y. H.; Song, K. D.; Park, H. G.; Jun, Y.; Yoo, P. J.; Park, J. H. Nanopatterned Conductive Polymer Films as a Pt, TCO-Free Counter Electrode for Low-Cost Dye-Sensitized Solar Cells. *Nanoscale* **2013**, *5*, 7838−7843.
(65) Yue, G.; Wu, J.; Xiao, Y.; Lin, J.; Huang, M.; Lan, Z.; Fan, L. Functionalized Graphene/Poly(3,4-ethylenedioxythiophene):Polystyrenesulfonate as Counter Electrode Catalyst for Dye-Sensitized Solar Cells. *Energy* **2013**, *54*, 315−321.
(66) Yun, D. J.; Ra, H.; Rhee, S. W. Concentration Effect of Multiwalled Carbon Nanotube and Poly(3,4-ethylenedioxythiophene) Polymerized with Poly(4-styrenesulfonate) Conjugated Film on the Catalytic Activity for Counter Electrode in Dye Sensitized Solar Cells. *Renewable Energy* **2013**, *50*, 692−700.